Vibration Analysis of Cracked Beams Using Adomian Decomposition Method and Non-Baseline Damage Detection via High-Pass Filters

Qibo Mao

School of Aircraft Engineering, Nanchang HangKong University, 696 South Fenghe Avenue, Nanchang, CN-330063, P. R. China

(Received 15 January 2014; accepted 20 October 2014)

The Adomian decomposition method (ADM) and high-pass filters are employed in this study to investigate the free vibrations and damage detection of cracked Euler-Bernoulli beams. Based on the ADM and employing some simple mathematical operations, the closed-form series solution of the mode shapes can be determined for beams consisting of an arbitrary number of cracks under general boundary conditions in a recursive way. Then, a high-pass filter is used to extract the irregularity profile from the corresponding mode shape. The location and size of the cracks in the beam can be determined by the peak value of the irregularity profile. The numerical results for different locations and depths of cracks on the damaged beam under different boundary conditions are presented. The results show that the proposed method is effective and accurate. The experimental work for aluminium cantilever beams with one and two cracks was performed to verify the proposed method. The successful detection of cracks in the beam demonstrates that the proposed method has great potential in crack detection of beam-type structures, as it is simple and does not require the mode shapes of an uncracked beam as a baseline.

1. INTRODUCTION

Recently, many vibration-based damage detection techniques have been developed due to their non-destructive nature.[1–3] The popularity of these techniques is based on the fact that the loss of stiffness due to structural damage changes the dynamic response of the structure. With these techniques, damages can be detected by monitoring the vibration parameters, such as damping ratios, natural frequencies, and mode shapes.

Mode shapes and/or their derivatives are generally used to predict the location and the size of the damage rather than natural frequencies. Because the natural frequencies are the global features of the structure, it is difficult to determine the damage location with a frequency-based method.[1] Since the 1990s, a lot of damage detection algorithms based on mode shape have been proposed for damage detection and localization.[1,2,4,5] Most of these methods require knowing the mode shapes of the health structures, which are difficult to obtain (and sometimes impossible), in order to establish a baseline for damage detection.

If the applicability of the mode shaped-based damage detection approach could be extended by eliminating the need for the baseline mode shapes, this approach would be significantly expanded in structural damage detection applications. Because of this potential, the non-baseline mode shape-based damage detection approaches have received more and more attention. Recently, Qiao and Cao[6] calculated the fractal dimension (FD) and waveform fractal dimension (WFD) of the mode shape from a cracked beam to determine the damage location and quantification. Ismail, et al.[7] used fourth derivatives of the mode shapes to directly identify the location of damage for reinforced concrete beams. The application of 1-D and 2-D wavelet transform methods to displacement mode shape for damage detection of beam and plate structures have also been extensively investigated.[8,9]

Ratcliffe, et al.[10,11] proposed the gapped smoothing method (GSM) and the global fitting method (GFM) for damage detection. The GSM and GFM do not require data from the undamaged structure. By applying GSM or GFM to the mode shapes of the damaged structures, a smoothing curve, which could be regarded as a substitution for the mode shape from the undamaged structure, can be extracted. The GSM and GFM later used the operating deflection shape and its curvature data, and were extended to directly use two-dimensional COS data for damage detections.[12–14]

Recently, Wang and Qiao[15] proposed an irregularity-based method to detect the cracks in beam structures. In this method, The Gaussian filter and triangular filter are applied on the mode shapes to extract the irregularities from the mode shape of the cracked beam, indicating the damage in the structure. The irregularity-based method was extended to detect the delamination in composite laminated beams and plates.[16,17]

In this study, high-pass filters are used to extract the irregularities from the mode shapes and determine the damage situation in a beam. The aim of the paper presented here is twofold. Firstly, mode shapes for a beam with an arbitrary number of cracks under general boundary conditions are determined by the Adomian decomposition method (ADM).[18–22] Using the

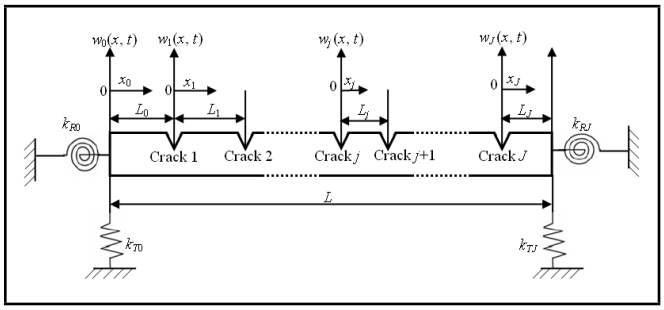

Figure 1. The coordinate system for a multiple-cracked beam, elastically restrained at both ends.

ADM, the governing differential equation for each section of the cracked beam becomes a recursive algebraic equation. The boundary conditions and continuity conditions at crack locations become simple algebraic frequency equations that are suitable for symbolic computation. Moreover, after some simple algebraic operations on these frequency equations, we can obtain the natural frequency and corresponding closed-form series solution of mode shape simultaneously.

As a second aim, this paper seeks to detect the location and depth of cracks in beam structures by using high-pass filters. The mode shapes are filtered by using a 3rd-order Butterworth high-pass filter, and their irregularities are extracted. The numerical calculation with different crack locations, depths, and number are discussed for a damaged beam under different boundary conditions. Finally, by using two aluminium cantilever beams with one and two cracks, the experimental damage detection was performed to verify the proposed method.

2. THE ADM FOR A CRACKED BEAM

Consider the free vibration of a uniform Euler-Bernoulli beam of length L consisting of J open cracks elastically restrained at both ends, as shown in Fig. 1. It is assumed that the cracks are located at $L_1, L_2, \ldots, L_{J-1}$, and $0 < L_1 < L_2 < \ldots < L_J < L$. The beam is divided into $(J+1)$ sections with the $(J+1)$ mirror systems of reference x_j $(j = 0, 1, \ldots, J)$.

The ordinary differential equation describing the free vibration in each section is as follows:

$$\frac{d^4\phi_j(x_j)}{dx_j^4} - \frac{m_s\omega^2}{EI}\phi_j(x_j) = 0,\ x_j \in [0, L_j],\ j = 0, 1, \ldots, J; \tag{1}$$

where subscript j denotes the beam between the jth crack and $(j+1)$th crack. $\phi_j(x_j)$ and ω are the structural mode shape and the natural frequency, respectively. E is Young's modulus. $I = \frac{bh^3}{12}$ is the cross-sectional moment of inertia of the beam. $m_s = \rho bh$ is the mass per unit length. ρ, b, and h are the density, width, and thickness of the beam, respectively.

Equation (1) can be rewritten in dimensionless form as follows:

$$\frac{d^4\Phi_j(X_j)}{dX_j^4} - \Omega^4\Phi_j(X_j) = 0, \quad X_j \in [0, R_j]; \tag{2}$$

where $X_j = \frac{x_j}{L}$, $\Phi_j(X_j) = \frac{\phi_j(x_j)}{L}$, $R_j = \frac{L_j}{L}$, $\Omega^4 = \frac{m_s\omega^2L^4}{EI}$, Ω is the dimensionless natural frequency, and the nth dimensionless natural frequency is denoted as $\Omega(n)$.

According to the ADM,[18–22] $\phi_j(X_j)$ in Eq. (2) can be expressed in terms of an infinite series

$$\Phi_j(X_j) = \sum_{m=0}^{\infty}\Phi_j^{[m]}(X_j); \tag{3}$$

where the component function $\Phi_j^{[m]}(X_j)$ will be determined recurrently.

If a linear operator $G = \frac{d^4}{dX^4}$ is imposed, the inverse operator of G is therefore a 4-fold integral operator defined by $G^{-1} = \int\int\int\int(\ldots)dXdXdXdX$, and

$$G^{-1}G\left[\Phi_j(X_j)\right] = \Phi_j(X_j) - \Phi_j(0) - \frac{d\Phi_j(0)}{dX_j}X_j - \frac{d^2\Phi_j(0)}{dX_j^2}\frac{X_j^2}{2} - \frac{d^3\Phi_j(0)}{dX_j^3}\frac{X_j^3}{6}. \tag{4}$$

Applying this on both sides of Eq. (2) with G^{-1}, we get

$$G^{-1}G\left[\Phi_j(X_j)\right] = \Omega^4G^{-1}\left[\Phi_j(X_j)\right] = = \Omega^4G^{-1}\left[\sum_{m=0}^{\infty}\Phi_j^{[m]}(X_j)\right]. \tag{5}$$

Comparing Eqs. (4) and (5), we get

$$\Phi_j(X_j) = \Phi_j(0) + \frac{d\Phi_j(0)}{dX_j}X_j + \frac{d^2\Phi_j(0)}{dX_j^2}\frac{X_j^2}{2} + \frac{d^3\Phi_j(0)}{dX_j^3}\frac{X_j^3}{6} + \Omega^4G^{-1}\left[\sum_{m=0}^{\infty}\Phi_j^{[m]}(X_j)\right]. \tag{6}$$

Finally, by using Eq. (3), the approximated solution of Eq. (6) can be determined by using the following recurrence relation:

$$\Phi_j^{[0]}(X_j) = \Phi_j(0) + \frac{d\Phi_j(0)}{dX_j}X_j + \frac{d^2\Phi_j(0)}{dX_j^2}\frac{X_j^2}{2} + \frac{d^3\Phi_j(0)}{dX_j^3}\frac{X_j^3}{6}; \tag{7}$$

$$\Phi_j^{[m]}(X_j) = \Omega^4G^{-1}\left[\Phi_j^{[m-1]}(X_j)\right]; \qquad m \geq 1. \tag{8}$$

By substituting Eqs. (7) and (8) into Eq. (3), and approximating the above solution by the truncated series, the following equation is found:

$$\Phi_j(X_j) = \sum_{m=0}^{M-1}\Phi_j^{[m]}(X_j) = = \sum_{s=0}^{3}\frac{d^s\Phi_j(0)}{dX^s}\sum_{m=0}^{M}\left[\Omega^{4m}\frac{X_j^{4m+n}}{(4m+n)!}\right]. \tag{9}$$

Equation (9) implies that $\sum_{m=M}^{\infty}\Phi_j^{[m]}(X_j)$ is negligibly small. The number of the series summation limit M is determined by convergence requirement in practice.

The unknown parameters $\frac{d^s\Phi_j(0)}{dX^s}$ $(s = 0, 1, 2, 3)$ and Ω in Eq. (9) can be determined based on the boundary condition

equations and the continuity conditions of each section of the beam.

The boundary conditions at the ends of the beam shown in Fig. 1 can be expressed in dimensionless form as follows:

$$\frac{d^2\Phi_0(0)}{dX_0^2} - K_{R0}\frac{d\Phi_0(0)}{dX_0} = 0,$$
$$\frac{d^3\Phi_0(0)}{dX_0^3} + K_{T0}\Phi_0(0) = 0; \quad (10)$$
$$\frac{d^2\Phi_J(R_J)}{dX_J^2} + K_{RJ}\frac{d\Phi_J(R_J)}{dX_J} = 0,$$
$$\frac{d^3\Phi_J(R_J)}{dX_J^3} - K_{TJ}\Phi_J(R_J) = 0; \quad (11)$$

where $K_{R0} = \frac{k_{R0}L}{EI}$, $K_{T0} = \frac{k_{T0}L^3}{EI}$, $K_{RJ} = \frac{k_{RJ}L}{EI}$, $K_{TJ} = \frac{k_{TJ}L^3}{EI}$, and $R_J = \frac{L_J}{L}$. k_{T0} and k_{TJ} are the stiffness of the translational springs, and k_{R0} and k_{RJ} are the stiffness of the rotational springs at $x_0 = 0$ and $x_J = L_J$, respectively.

Substituting Eq. (9) into Eq. (10), the mode shape function for the first section $\Phi_0(X_0)$ can be expressed as a linear function of $\Phi_0(0)$ and $\frac{d\Phi_0(0)}{dX_0}$, as follows:

$$\Phi_0(X_0) = \Phi_0(0)\left\{\sum_{m=0}^{M-1}\left[\Omega^{4m}\frac{X_0^{4m}}{(4m)!}\right] - K_{T0}\sum_{m=0}^{M-1}\left[\Omega^{4m}\frac{X_0^{4m+3}}{(4m+3)!}\right]\right\} + \frac{d\Phi_0(0)}{dX_0}\left\{\sum_{m=0}^{M-1}\left[\Omega^{4m}\frac{X_0^{4m+1}}{(4m+1)!}\right] + K_{R0}\sum_{m=0}^{M-1}\left[\Omega^{4m}\frac{X_0^{4m+2}}{(4m+2)!}\right]\right\}. \quad (12)$$

Due to the localized crack effect, the crack of the beam can be simulated as a massless spring.[6] For each crack between the two sections, conditions can be introduced which impose continuity of displacement, bending moment, and shear. Moreover, an additional condition imposes equilibrium between the transmitted bending moment and the rotation of the spring representing the crack. Consequently, the continuity conditions in dimensionless form are[6,8]

$$\Phi_{j+1}(0) = \Phi_j(R_j),$$
$$\frac{d\Phi_{j+1}(0)}{dX_{j+1}} = \frac{d\Phi_j(R_j)}{dX_j} + \theta_j\frac{d^2\Phi_j(R_j)}{dX_j^2}; \quad (13)$$
$$\frac{d^2\Phi_{j+1}(0)}{dX_{j+1}^2} = \frac{d^2\Phi_j(R_j)}{dX_j^2},$$
$$\frac{d^3\Phi_{j+1}(0)}{dX_{j+1}^3} = \frac{d^3\Phi_j(R_j)}{dX_j^3}; \quad (14)$$

where θ_j is the dimensionless jth crack flexibility. $\theta_j = 5.346h \cdot J\left(\frac{a_j}{h}\right)$ and a_j is the depth of the jth crack. $J\left(\frac{a_j}{h}\right)$ is the dimensional local compliance function,[6,15] given by

$$J\left(\frac{a_j}{h}\right) = 1.8624r_j^2 - 3.95r_j^3 + 16.37r_j^4 - 37.226r_j^5 + 76.81r_j^6 - 126.9r_j^7 + 172r_j^8 - 43.97r_j^9 + 66.56r_j^{10}; \quad (15)$$

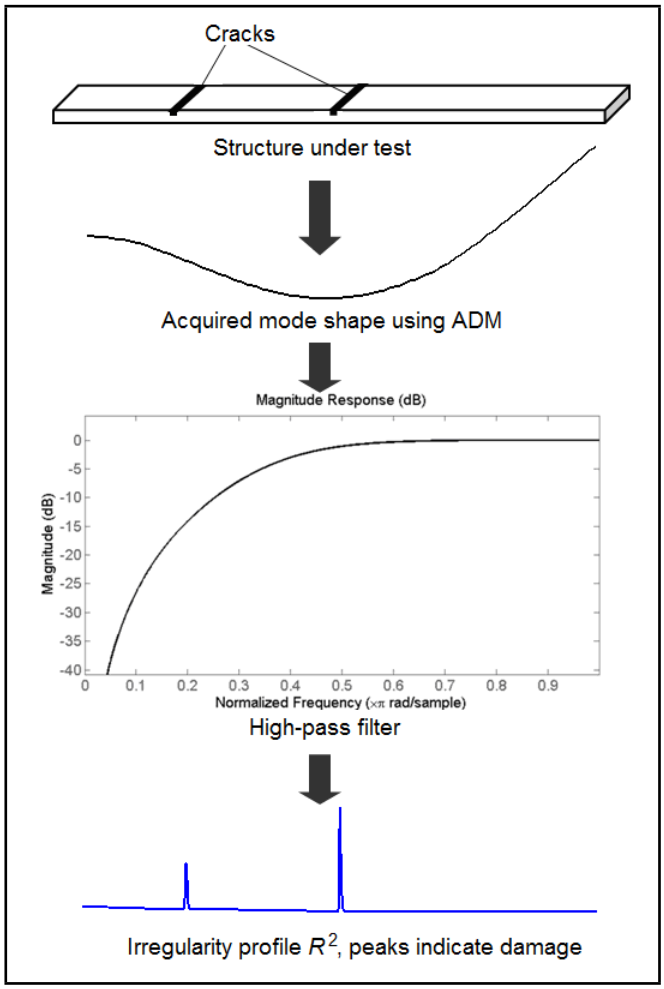

Figure 2. Damage detection procedure using high-pass filter.

where r_j is the dimensionless depth of the jth crack, $r_j = \frac{a_j}{h}$.

Substituting Eqs. (13) and (14) into Eq. (9), the mode shapes for the section-j ($j \geq 0$) can be written as

$$\Phi_{j+1}(X_{j+1}) = \Phi_j(R_j)\sum_{m=0}^{M-1}\left[\Omega^{4m}\frac{X_{j+1}^{4m}}{(4m)!}\right] + \left[\frac{d\Phi_j(R_j)}{dX_j} + \theta_j\frac{d^2\Phi_j(R_j)}{dX_j^2}\right]\sum_{m=0}^{M-1}\left[\Omega^{4m}\frac{X_{j+1}^{4m+1}}{(4m+1)!}\right] + \frac{d^2\Phi_j(R_j)}{dX_j^2}\sum_{m=0}^{M-1}\left[\Omega^{4m}\frac{X_j^{4m+2}}{(4m+2)!}\right] + \frac{d^3\Phi_j(R_j)}{dX_j^3}\sum_{m=0}^{M-1}\left[\Omega^{4m}\frac{X_{j+1}^{4m+3}}{(4m+3)!}\right]. \quad (16)$$

Notice that there are only three unknown parameters ($\Phi_0(0)$, $\frac{d\Phi_0(0)}{dX_0}$, and Ω) in Eq. (16) in a recursive way. By substituting Eqs. (16) into Eqs. (11) and (12), this boundary condition equation can be expressed as linear functions of $\Phi_0(0)$ and $\frac{d\Phi_0(0)}{dX_0}$, such as

$$f_{11}(\Omega)\Phi_0(0) + f_{12}(\Omega)\frac{d\Phi_0(0)}{dX_0} = 0; \quad (17)$$
$$f_{21}(\Omega)\Phi_0(0) + f_{22}(\Omega)\frac{d\Phi_0(0)}{dX_0} = 0. \quad (18)$$

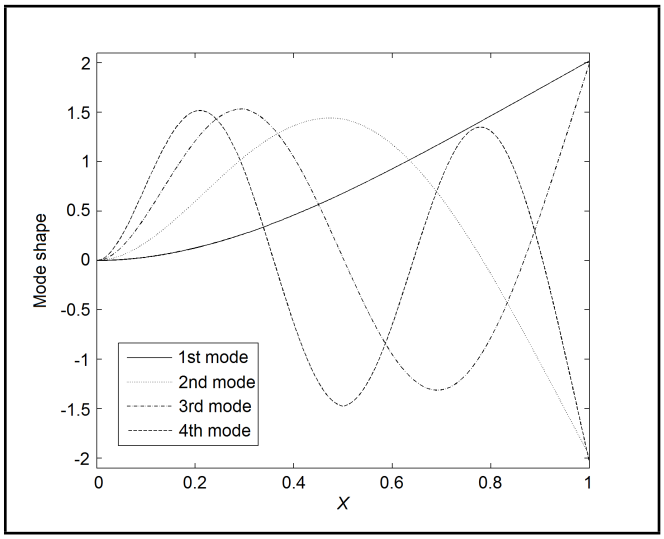

Figure 3. The first four mode shapes of the cantilever beam with two cracks.

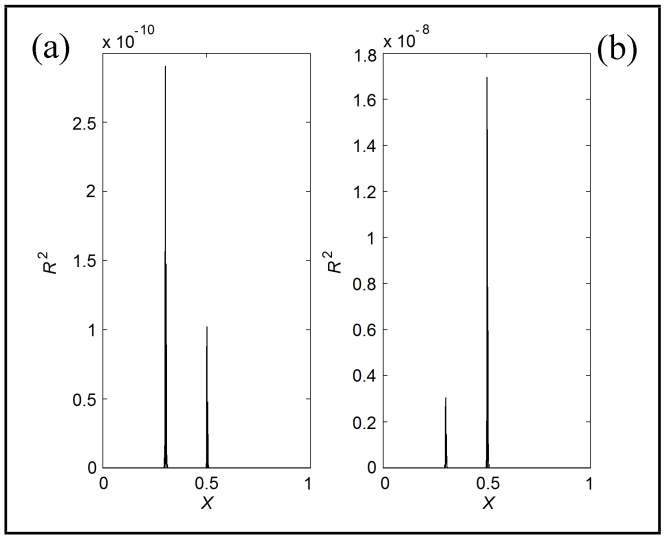

Figure 4. The irregularity profile R^2 for (a) the first mode shape; (b) the second mode shape.

From Eqs. (17) and (18), the dimensionless natural frequency Ω can be solved by

$$f_{11}(\Omega)f_{22}(\Omega) - f_{12}(\Omega)f_{21}(\Omega) = \sum_{n=0}^{N} S_n \Omega^n = 0. \qquad (19)$$

Notice that Eq. (19) is a polynomial of degree N evaluated at Ω. By using the functions `sym2poly` and `roots` in the MATLAB Symbolic Math Toolbox, Eq. (19) can be directly solved. The next step is to determine the nth mode shape function corresponding to the nth dimensionless natural frequency $\Omega(n)$. Substituting the solved $\Omega(n)$ into Eq. (17) or (18), the unknown parameter $\frac{d\Phi_0(0)}{dX_0}$ can be expressed as the function of $\Phi_0(0)$, as follows:

$$\frac{d\Phi_0(0)}{dX_0} = -\frac{f_{11}(\Omega)}{f_{12}(\Omega)}\Phi_0(0) = -\frac{f_{21}(\Omega)}{f_{22}(\Omega)}\Phi_0(0). \qquad (20)$$

Substituting Eq. (20) into Eqs. (12) and (16), the mode shape function for each section can be obtained. The mode shape function for the entire beam can be written as

$$\Phi(X) = \left[\Phi_0(X_0) \;\; \Phi_1(X_1) \;\; \ldots \;\; \Phi_J(X_J)\right]. \qquad (21)$$

It should be noted that the proposed method can be used to analyse the vibration of beams consisting of an arbitrary number of cracks in a recursive way, and the complexity of the vibration is the same order of a uniform beam without any cracks. The solution can be obtained by solving a set of algebraic equations with only three unknowns, and the resultant problem is significantly simpler compared to the one obtained through a traditional way.

3. DAMAGE DETECTION USING HIGH-PASS FILTER

It has been demonstrated that the mode shapes of the damage structures consist the irregularities induced by the damage. The mode shapes of the damage structures $\Phi(x)$ can be expressed as

$$\Phi(x) = \Phi_h(x) + R(x); \qquad (22)$$

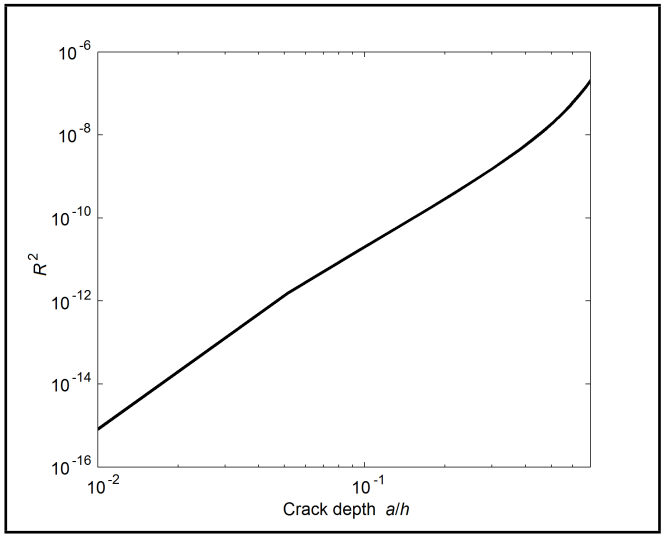

Figure 5. The peak R^2 value of the first mode varies with the second crack depth.

where $\Phi_h(x)$ is the mode shape for the health structure, $R(x)$ is the irregularity curve due to the damage, and $R^2(x)$ is termed as the irregularity profile,[15] which is used as a damage index (DI) throughout this study.

However, it is impossible to directly observe the irregularity profile R^2 from the mode shape only. The irregularities on the mode shapes should be amplified and separated to determine the locations and sizes of damages. In this study, the irregularities on the mode shapes are extracted through the separation of damage information in frequency domain rather than traditional spatial domain. It was found that the irregularities due to damage create an additional high-frequency component in the amplitude spectrum of the mode shapes that is not present in the health structures.[23] This means that it is possible to extract the irregularities of the mode shapes by using high-pass filters. The basic idea of the damage detection procedure is shown in Fig. 2.

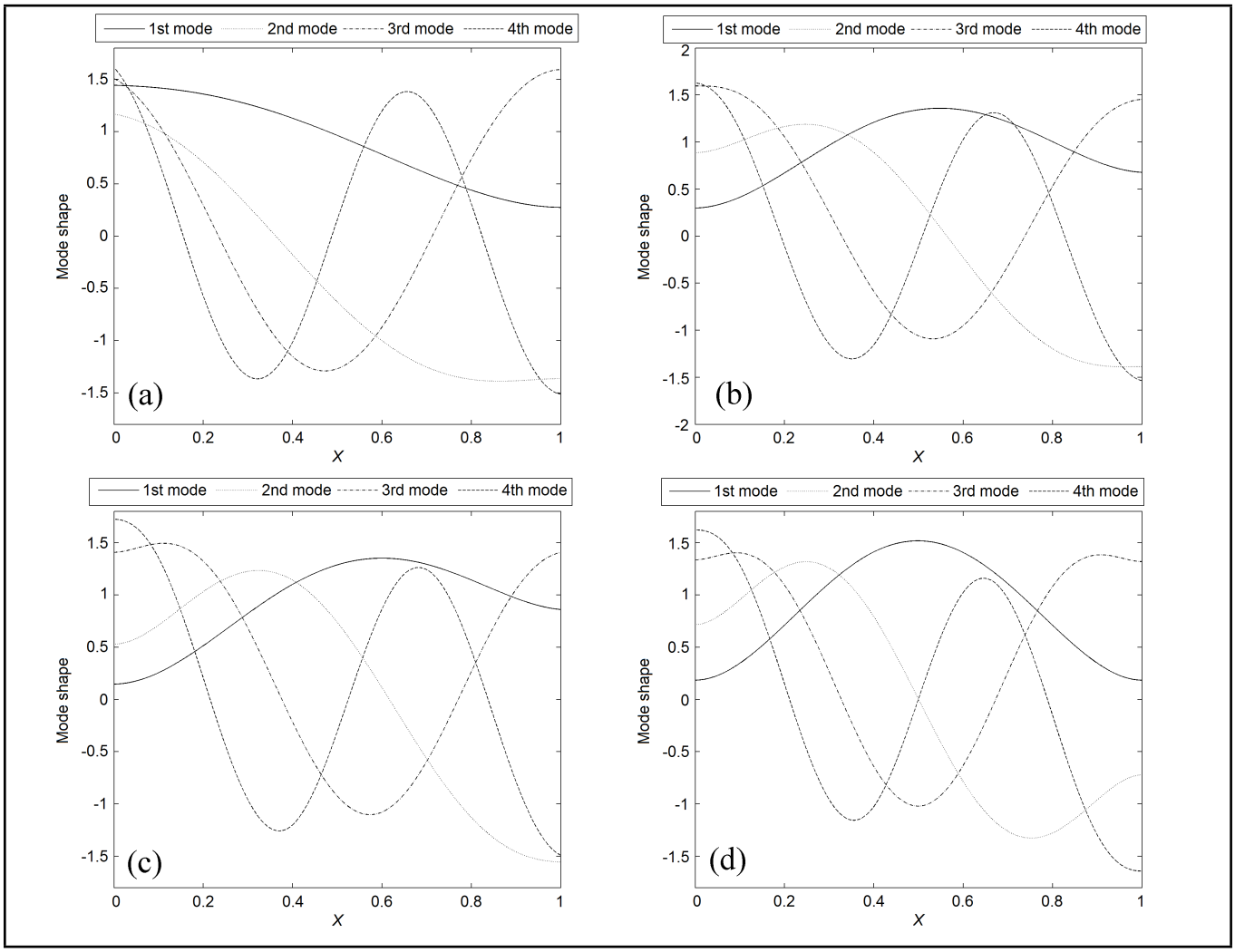

Figure 6. The first four mode shapes for the two-cracked beam with different boundary conditions (Other parameters listed in Table 1): (a) $K_{T0} = 10$, $K_{R0} = 20$, $K_{TJ} = 100$, $K_{RJ} = 200$; (b) $K_{T0} = 400$, $K_{R0} = 300$, $K_{TJ} = 200$, $K_{RJ} = 100$; (c) $K_{T0} = 700$, $K_{R0} = 600$, $K_{TJ} = 150$, $K_{RJ} = 50$; (d) $K_{T0} = K_{R0} = K_{TJ} = K_{RJ} = 1000$.

4. NUMERICAL CALCULATIONS

4.1. A Cantilever Beam with Two Cracks

In order to verify the proposed method for damage detection, a cantilever aluminium beam with two cracks at a distance of $0.3L$ and $0.5L$ from the clamped end, respectively, is considered firstly. The relative depths of these two cracks are the same and chosen as $a/h = 0.1$. The beam under analysis has the following properties: length $L = 0.51$ m, rectangular cross-section with width $b = 0.03$ m, and thickness $h = 0.004$ m. A 3rd-order high-pass Butterworth filter is used to extract the irregularity profile. Figure 3 shows the first four mode shapes for the cracked beams. From Fig. 3, no effects from the cracks can be observed in the mode shape. Figure 4 shows the extracted irregularities profile R^2 of the first and second modes. From Fig. 4, it can be found that the locations of the cracks can be determined using the irregularity profile.

To study the ability of the proposed method to detect crack depth, it was assumed that the location and depth of the first crack location are $R_1 = 0.1$ and $r_1 = 0.1$, respectively. Figure 5 shows the effect of the depths of the peak R^2 values of the first mode at the second crack location. From Fig. 5, it can be seen that the peak R^2 value is larger when the crack depth is increased. This means that the peak R^2 value can be applied as a criterion for crack depth.

4.2. Two Cracks Beam under General Boundary Conditions

Because the proposed method based on the ADM technique offers a unified and systematic procedure for vibration analysis of the cracked beam with arbitrary boundary conditions, the calculation of the natural frequencies and corresponding mode shapes for different boundary conditions can be very easy. For example, the modification of boundary conditions from one case to another is as simple as changing the values of the stiffness of translational and rotational springs. And it does not involve any changes to the solution procedures or algorithms. Table 1 lists the first four dimensionless natural frequencies $\Omega(n)$ for the beam with two cracks with different boundary conditions. Figure 6 shows the first four corresponding mode shapes for the cracked beams listed in Table 1. Figure 7 shows the extracted irregularities profile R^2 of the first mode under different boundary conditions. In all cases, the cracks can be

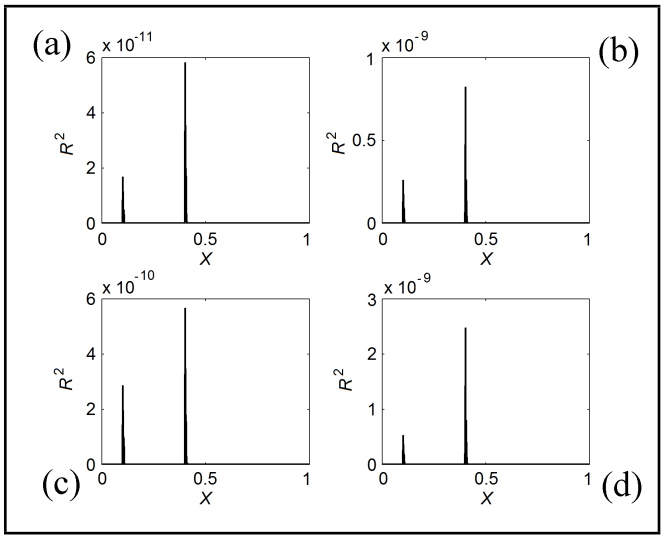

Figure 7. The irregularities profile R^2 of the first mode under different boundary conditions shown in Fig. 6.

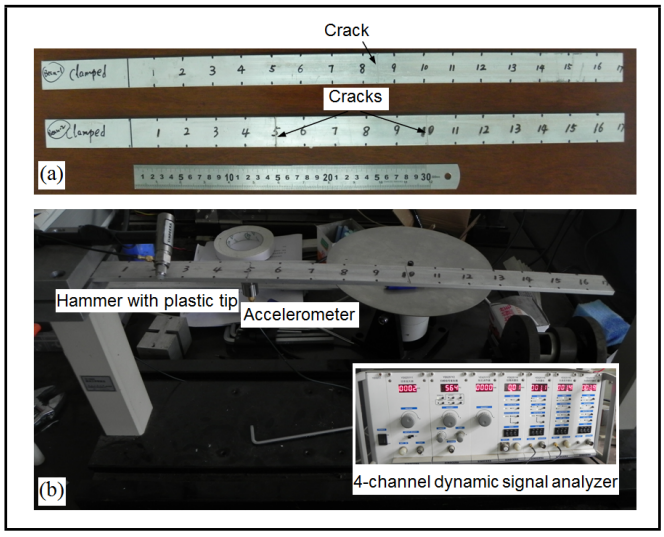

Figure 8. Photographs of (a) the cantilever beams; (b) experiment setup in the laboratory.

easily detected from the irregularity profiles.

5. EXPERIMENTAL VERIFICATION

5.1. Experiment Setup

To verify the above damage detection results, a set of laboratory experiments was performed to examine its effectiveness for real measurement data. Two applications including the cantilever beams with one crack and two cracks are illustrated. Two aluminium cantilever beams with dimensions $600 \times 30 \times 4$ mm, Young's modulus $E = 70 \times 10^9$ Pa, and density $\rho_s = 2700$ kg/m^3 are fabricated. The beams were clamped at one end and free at the other, and the effective length of both beams is 510 mm, as shown in Fig. 8(a). The cracks were made using a saw cut. The crack is located at 255 mm from the clamped end for the one-crack beam, and the crack locations are at 150 mm and 300 mm from the clamped end for the other beam. The depth of all through-width cut is about 1–1.5 mm.

It is well known that there are two methods for modal test using the impact hammer, i.e. a roving hammer or a roving accelerometer. In this study, all experiments were carried out with the roving impact hammer. The beams were excited by a moving hammer from Sinocera Piezotronics, Inc. (Yangzhou, China) with a plastic tip and a force transducer (with the sensitivity of 4 pC/N and a load range of 0–2000 N) at 17 points, equally spaced (every 30 mm) along the length of the beam. The excitation points were numbered from 1 to 17, starting from the fixed end. An accelerometer from Sinocera Piezotronics, Inc. with the weight of 28 g, sensitivity of 50 pC/g, and a frequency range of 0.5–6000 Hz is mounted at the opposite side of the 5th hammer excitation point (the distance of 150 mm from the clamped end) to measure the response of the beams. A SINOCERA dynamic signal analyser (with 4 channels, but only 2nd and 3rd channel used) is used to acquire the frequency response functions between force and the accelerations, as shown in Fig. 8(b). The square and exponential windows were used to filter the force and acceleration signals, respectively. Three measurements were taken for each impact location to help minimize variance errors. Finally, the post-processing software (N-MODAL) was used to obtain the modal parameters such as natural frequencies, damping ratios, and mode shapes. N-MODAL software contains two built-in curve-fitting methods: Peak Fit and Polynomial Fit. The Polynomial Fit method was used to extract the experimental modal parameters.

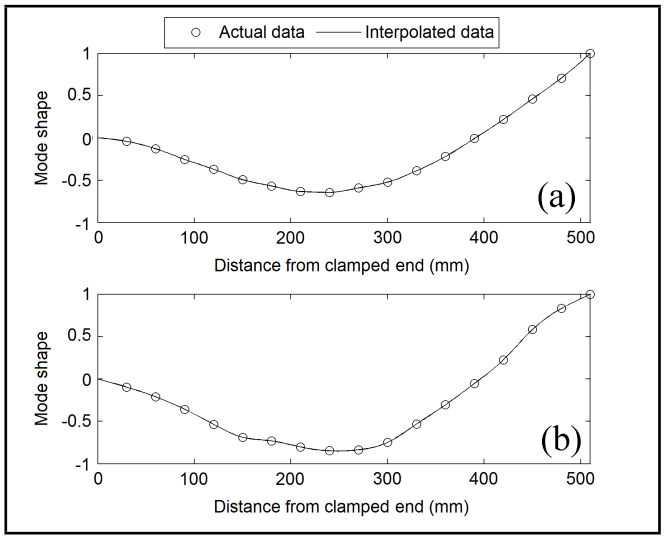

Figure 9. The interpolated mode shapes for the beam (a) with one crack at 255 mm, and (b) with two cracks at 150 mm and 300 mm.

5.2. Experimental Results

In brief, only the second measured modes of the beam with one and two cracks are used to extract the irregularity profile R^2. Notice that there are only 17 experimental measurement points, and if the high-pass filter is directly implemented, many points of the sample data would be detected as singularities. In this study, a cubic spline interpolation technique is applied to smooth the transition from one point to another. As a result, a total number of 200 interpolated points is obtained. Figure 9

Table 1. The first four dimensionless natural frequencies $\Omega(n)$ for a two-cracks beam under different boundary conditions (crack location $R_1 = 0.1$, $R_2 = 0.4$; crack depth $r_1 = 0.1$, $r_2 = 0.15$).

Stiffness of springs (Boundary conditions)				Mode index			
K_{T0}	K_{R0}	K_{TJ}	K_{RJ}	1	2	3	4
10	20	100	200	2.602601	4.221255	6.381824	9.281358
400	300	200	100	4.054168	5.662266	7.367550	9.749038
700	600	150	50	3.980091	5.712174	7.701976	9.916163
1000	1000	1000	1000	4.518749	6.915724	8.752670	10.635948

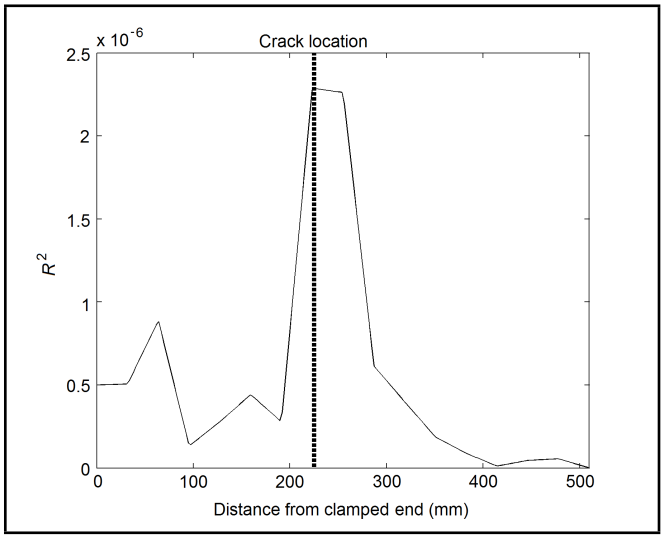

Figure 10. The irregularity profile R^2 for the beam with one crack at 255 mm.

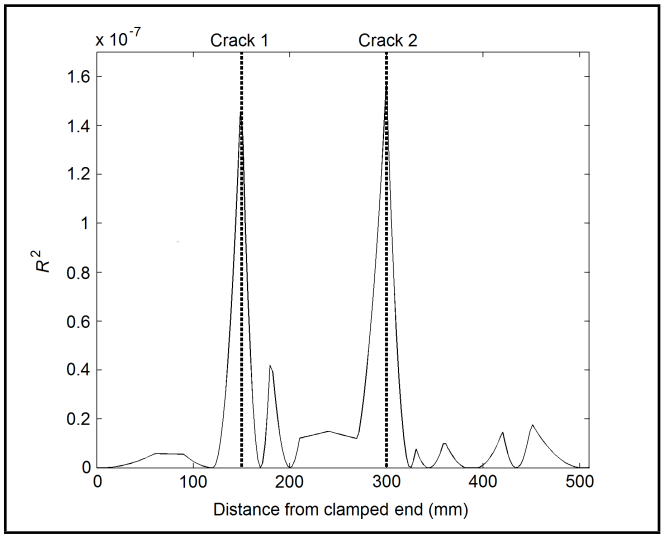

Figure 11. The irregularity profile R^2 for the beam with two cracks at 150 mm and 300 mm.

shows the interpolated mode shapes of the beam.

By using 3rd-order high-pass Butterworth filter, the irregularity profiles R^2 for the mode shapes shown in Fig. 9 are obtained and presented in Figs. 10 and 11. From Figs. 10 and 11, it can be seen that the largest peak values appear at the crack locations. This means that the proposed method based on high-pass filters can successfully detect the damage in actual tests.

6. CONCLUSIONS

In this study, the vibration of Euler-Bernoulli beams under different boundary conditions with an arbitrary number of cracks are analysed in a recursive way based on the Adomian decomposition method (ADM). Then the high-pass filters are introduced to detect the damage for beams under different boundary conditions. In this method, the mode shapes can be filtered and their irregularities due to damage are extracted. Furthermore, it is possible to determine the depth of a crack in beams by the peak value at the crack location of the irregularity profile. The main advantage of the proposed method is that the information of the undamaged structure is not required. To further validate the proposed method, the experimental damage detection was investigated using two aluminium cantilever beams with one and two cracks, respectively. The results demonstrate favourable feasibility and effectiveness of the proposed damage detection method.

ACKNOWLEDGEMENTS

This work was sponsored by the National Natural Science Foundation of China (no. 51265037, no. 11464031), the Technology Foundation of Jiangxi Province, China (no. KJLD12075), and the Aeronautical Science Foundation of China (no. 2015ZA56002)..

REFERENCES

[1] Adewuyi, A. P., Wu, Z., and Serker, N. H. M. K. Assessment of vibration-based damage identification methods using displacement and distributed strain measurements, *Structural Health Monitoring*, **8** (6), 443–461, (2009).

[2] Fan, W. and Qiao, P. Vibration-based damage identification methods: a review and comparative study, *Structural Health Monitoring*, **10** (1), 83–111, (2011).

[3] Salawu, O. S. Detection of structural damage through changes in frequency: a review, *Engineering Structures*, **19** (9), 718–723, (1997).

[4] Pandey, A. K., Biswas, M., and Samman, M. M. Damage detection from changes in curvature mode shapes, *Journal of Sound and Vibration*, **145** (2), 321–332, (1991).

[5] Wahab, M. M. A. and Roeck, G. D. Damage detection in bridges using modal curvatures: application to a real damage scenario, *Journal of Sound and Vibration*, **226** (2), 217–235, (1999).

[6] Qiao, P. and Cao, M. Waveform fractal dimension for mode shaped-based damage identification of beam-type structures, *International Journal of Solids and Structures*, **45** (22–23), 5946–5961, (2008).

[7] Ismail, Z., Razak, H. A., and Rahman A. G. A. Determination of damage location in RC beams using mode shape derivatives,. *Engineering Structures*, **28**, 1566–1573, (2006).

[8] Zhong, S. and Oyadiji, S. O. Crack detection in simply supported beams without baseline modal parameters by stationary wavelet transform, *Mechanical Systems and Signal Processing*, **21** (4), 1853–1884, (2007).

[9] Fan W. and Qiao, P. A 2-D continuous wavelet transform of mode shape data for damage detection of plate structures, *International Journal of Solids and Structures*, **46** (25–26), 4379–4395, (2009).

[10] Ratcliffe, C. and Bagaria W. Vibration technique for locating delamination in a composite beam, *AIAA Journal*, **36** (6), 1074–1077, (1998).

[11] Ratcliffe, C. P. A frequency and curvature based experimental method for locating damage in structures, *ASME Transaction Journal of Vibration and Acoustics*, **122** (3), 324–329, (2000).

[12] Yoon, M. K., Heider, D., Gillespie, J .W., Ratcliffe, C. P., and Crane, R. M. Local damage detection using the two-dimensional gapped smoothing method, *Journal of Sound and Vibration*, **279** (1–2), 119–139, (2005).

[13] Yoon, M. K., Heider, D., Gillespie, J. W., Ratcliffe, C. P., and Crane, R. M. Local damage detection with the global fitting method using mode shape data in notched beams, *Journal of Non-destructive Evaluation*, **28** (2), 63–74, (2009).

[14] Zhang, Y., Lie, S. T., and Xiang, Z. Damage detection method based on operating deflection shape curvature extracted from dynamic response of a passing vehicle, *Mechanical System and Signal Processing*, **35**, 238–254, (2013).

[15] Wang, J. and Qiao P. On irregularity-based damage detection method for cracked beam, *International Journal of Solids and Structures*, **45**, 688–704, (2008).

[16] Bazardehi, S. R. K. and Kouchakzadeh, M. A. Detection of delamination in cross-ply composite-laminated beams utilizing irregularity of mode shapes, *Proceedings of the IMechE, Part G: Journal of Aerospace Engineering*, **225** (12), 1302–1309, (2011).

[17] Bazardehi, S. R. K. and Kouchakzadeh, M. A. Detection of delamination in composite laminated plates using filtered mode shapes, *Proceedings of the IMechE, Part C: Journal of Mechanical Engineering Science*, **226** (12), 2902–2911, (2012).

[18] Adomian G. *Solving frontier problems of physics: the decomposition method*, Kluwer-Academic Publishers, Boston, (1994).

[19] Mao, Q. and Pietrzko, S. Design of shaped piezoelectric modal sensor for beam with arbitrary boundary conditions by using Adomian decomposition method, *Journal of Sound and Vibration*, **329**, 2068–2082, (2010).

[20] Mao, Q. Free vibration analysis of elastically connected multiple-beams by using the Adomian modified decomposition method, *Journal of Sound and Vibration*, **331** (11), 2532–2542, (2012).

[21] Mao, Q. Free vibration analysis of multiple-stepped beams by using Adomian decomposition method, *Mathematical and Computer Modelling*, **54** (1–2), 756–764, (2012).

[22] Mao, Q. and Pietrzko, S. Free vibration analysis of a type of tapered beams by using Adomian decomposition method, *Applied Mathematics and Computation*, **219** (6), 3264–3271, (2012).

[23] Sazonov, E. S., Klinkhachorn, P., Halabe, U. B., and Gangarao, H. V. S. Non-baseline detection of small damages from changes in strain energy mode shapes, *Nondestructive Testing and Evaluation*, **18** (3–4), 91–107, (2003).